Protective Effects of DAla2-GIP-GLU-PAL against Cognitive Deficits and Amyloid Deposition in APP/PS1 AD Mice Associated with Reduction of Neuroinflammation

Li Yuan
Department of Physiology, Changzhi Medical College

Jun Zhang
Department of Physiology, Key laboratory of Cellular Physiology, Ministry of Education, Shanxi Medical University

Christian Holscher
Research and Experiment Center, Henan University of Chinese Medicine

Jun-Ting Yang
Department of Physiology, Key Laboratory of Celluar Physiology, Ministry of Education,Shanxi Medical University

Mei-Na Wu
Department of Physiology, Key Laboratory of Cellular Physiology, Ministry Education, Shanxi Medical University

Zhao-Jun Wang
Department of Physiology, Key Laboratory of Celluar Physiology, Ministry of Education, Shanxi Medical University

Hong-Yan Cai
Department of Immunology and Microbiology, Shanxi Medical Yniversity

Ling-Na Han
Department of Physiology, Changzhi Medical College

Hui Shi
Department of Physiology, Key Laboratory of Cellular Physiology, Ministry of Education, Shanxi Medical University

Yu-Fei Han
Department of Physiology, Key Laboratory of Cellular Physiology, Ministry of Education, Shanxi Medical University

Jinshun Qi (jinshunqi2009@163.com)
shanxi medical university https://orcid.org/0000-0001-9223-8806

Research

Keywords: DAla2GIP-Glu-PAL, Cognitive behaviors, Long-term synaptic plasticity, Amyloid-β (Aβ), Neuroinflammation, cAMP/PKA/CREB, APP/PS1 mice

Posted Date: April 16th, 2020

DOI: https://doi.org/10.21203/rs.3.rs-22108/v1

Abstract

Background Alzhermer's disease (AD) is a neurodegenerative disease characterized by progressive decline in cognitive function and high-density deposition of amyloid-β (Aβ) plaques in the brain. Type 2 diabetes mellitus (T2DM) is an important risk factor for AD. Glucose-dependent insulinotropic polypeptide (GIP) has been identified to be effective in T2DM treatment and neuroprotection. The present study further investigated the neuroprotective effects of a novel long lasting GIP analogue DAla2GIP-Glu-PAL in 9-month-old APP swe /PS1 dE9 (APP/PS1) AD mice. Methods Multiple behavioral tests including new object recognition, Y maze and Morris water maze were performed to examine the cognitive function of mice. In vivo hippocampal late-phase long-term potentiation (L-LTP) was recorded to reflect synaptic plasticity. Immunohistochemistry and immunofluorescence were used to examine the Aβ plaques and neuroinflammation in the brain. The expression levels of cAMP, S99 p-PKA, S133 p-CREB, S468 NF-κBp65 and IL-1β were detected by western blotting or ELISA. Results DAla2GIP-Glu-PAL effectively improved cognitive behaviors and synaptic plasticity of APP/PS1 mice, with increased new object recognition, spontaneous alternation and target quadrant swimming time, as well as enhanced in vivo hippocampal L-LTP. DAla2GIP-Glu-PAL significantly reduced Aβ deposition and inhibited astrocyte proliferation, IL-1β secretion and NF-κB activation. Besides, . DAla2GIP-Glu-PAL also up-regulated cAMP/PKA/CREB signal transduction in the hippocampus of APP/PS1 mice. Conclusion DAla2GIP-Glu-PAL improves cognitive behaviors, long-term synaptic plasticity and pathological damages in APP/PS1 mice, which are associated with the reduction of neuroinflammation and the up-regulation of cAMP/PKA/CREB signaling in the hippocampus. This study suggests a potential benefit of DAla2GIP-Glu-PAL in the treatment of AD.

Introduction

Alzhermer' disease (AD) is a progressive neurodegenerative disease in the central nervous system. According to World Alzheimer's Disease Report 2018, dementia afflicts more than 47 million people worldwide, and this number will increase to 152 million by 2050[1]. However, there is no effective drug to stop the AD process. It is well known that the main pathological hallmarks in the AD brain are high-density of amyloid-β (Aβ) plaques and neurofibrillary tangles (NFTs), as well as progressive neuronal loss and brain atrophy[2]. Aβ deposition in the brain may be the basis for the pathological changes in AD, which triggering tau protein hyperphosphorylation and ultimate neuronal degeneration. It has been reported that intracerebral ventricular[3] or intra-hippocampal[4] injection of Aβ suppressed late-phase long-term potentiation (L-LTP) of synaptic transmission in the hippocampal CA1 region of rats; Aβ damaged spatial learning and memory behavior in rats[5]; and Aβ evoked neuroinflammation in the hippocampus[6, 7]. Further, inflammatory factors such as interleukin 1 beta (IL-1β) and TNF-α could accelerate Aβ deposition[8, 9]. Therefore, it is still a promising strategy for the treatment of AD by preventing Aβ accumulation and neuroinflammatory response.

Type 2 diabetes mellitus (T2DM) is an important risk factor for AD[10, 11]. Several studies have shown close association between abnormal glucose and insulin metabolism and the development of AD[12, 13]. Talbot et al. [14] confirmed that insulin signaling was severely desensitized in the brain of AD patients,

even in non-diabetic patients. Insulin is a key growth factor which not only regulates energy metabolism but also affects structural and functional integrity of synapses in the central nerves system[15]. A recent clinical study demonstrated that long-acting intranasal insulin improves cognition for adults with mild cognitive impairment or early-stage AD dementia[16]. In view of the similarities and close association between AD and T2DM, drugs originally developed for T2DM treatment such as insulin have been tested as potential treatments for AD. However, the desensitization of the insulin receptor has been discovered in the brain of AD patients[17], which is one of the underlying mechanisms of neurodegeneration in AD. So, it is not sensible to give insulin administration to people with AD. Moreover, chronic administration of insulin has dangerous effects on blood sugar levels in the AD patients[16]. Glucose-dependent insulinotropic polypeptide (GIP), a 42-amino acid incretin growth factor, is a potential candidate in the treatment of AD as it activates a parallel signaling pathway to insulin[18]. GIP modulates the insulin-signaling pathway intracellularly, rather than directly facilitats insulin receptor expression. Meantime, the glucose-dependency of GIP make it more safe for the AD patients with normal blood glucose level[19]. GIP receptors are expressed in the brain especially on larger neurons such as the cerebral cortex and hippocampal pyramidal neurons[20]. Moreover, the neuroprotective and regenerative properties of GIP have been reported[21]. For example, GIP prevents the detrimental effects of Aβ on synaptic plasticity[22] and spatial learning and memory during water maze task[23]; GIP promote axonal regeneration after sciatic nerve injury[20]. However, endogenous GIP can be quickly degraded by the enzyme dipeptidyl peptidase IV (DPP-IV), with only 2 minutes of biological half-life [24]. Luckily, several enzyme-resistant super-GIP molecules have been designed, such as DAla2GIP[18] and DAla2-GIP-GLU-PAL[25], which have a significantly extended half-life to several hours. Moreover, our previous studies have shown that DAla2GIP could cross the blood brain barrier[26, 27]. DAla2-GIP-GLU-PAL, a structure-modified peptide of DAla2GIP with higher resistance to DPP-IV cleavage and stronger lipid solubility, has shown neuroprotective roles in a chronic Parkinson's disease mouse model after intraperitoneal (i. p.) injection[28]. Therefore, it will be interesting to test whether this novel GIP analogue has neuroprotective properties in the AD animal model.

In the present study, we explored the effects of DAla2-GIP-glu-PAL on the cognitive behaviors in 9-month-old APP/PS1 transgenic mouse model of AD by using multiple behavioral tests. Further, we examined the pathological features in the brain of AD mice and investigated electrophysiological and molecular mechanisms by recording in vivo hippocampal late phase LTP (L-LTP) and measuring neuroinflammatory responses and cAMP/PKA/CREB pathway in the hippocampus of APP/PS1mice.

Materials And Methods

Animals and treatments

Heterozygous male APPswe/PS1dE9 (APP/PS1) mice with a C57BL/6J background and wild-type (WT) littermates were purchased from the Institute of Laboratory Animal Sciences (SCXX: 2013 -0002) and bred at the Research Animal Center of Shanxi Medical University with approval of the Shanxi Committee on Ethics of Animal Research. Animals were kept in a room with controlled temperature (20–24℃),

humidity (60–80%), light-dark cycle (12/12 hr) and free access to standard rodent chow and water. The APP/PS1 and WT mice were randomly divided into four groups: WT + PBS, APP/PS1 + PBS, WT + DAla2GIP-Glu-PAL, and APP/PS1 + DAla2GIP-Glu-PAL (*n* = 12 in each group).

Peptides and Drug treatment

DAla2GIP-Glu-PAL was presented by Professor Christian Holscher of Lancaster University, UK. The powdery DAla2GIP-Glu-PAL was dissolved in 0.01 M PBS solution at a final concentration of 5 μM, and stored in a refrigerator at -20 °C after dispensing. APP/PS1 and WT mice were intraperitoneally injected with PBS (0.01M) or DAla2GIP-Glu-PAL (5 μM) at a volume of 0.2 ml once a day for three weeks prior to behavioral study, maintaining the injection during all the behavioral tests.

New object recognition test in open field

New object recognition test was performed in an open field. The apparatus consisted of an open field arena (length, 55 cm; width, 55 cm; height, 30 cm). Each mouse was placed in the middle of the open-field and was allowed to freely explore for 5 min. All behaviors of mice were recorded by an infrared camera fixed 2 m above the center point of the open-field. The camera was connected to a video recorder, monitor and a computer. The movement traces and running distance of the animals in the open-field were analyzed by the Ethovision 3.0 software system (Noldus Information Technology, Wageningen, the Netherlands). In new object recognition test, mice were firstly subject to a 10 min acquisition trial, during which they were placed in the open-field in the presence of two identical objects (cubes) situated at 15 cm from the arena wall (acquisition task). On completion of 10 min exploration, the mouse was returned to its cage for a 3 h delay. Then, the mouse was placed back and exposed to one familiar object (cube) and a novel object (ball) for 10 min (test task). The objects were placed in the same locations as the objects in the previous acquisition task. The total time spent for exploring each object (when the animal's snout was directly toward the object at a distance ≤ 2 cm) was recorded, and the recognition index (RI) was defined as the amount of time exploring the novel object over the total time spent exploring both objects times [(time exploring the novel object/total time exploring both objects) × 100%]. A higher RI indicates greater memory retention. In the acquisition and test tasks, if the exploration time was < 30 s and < 15 s, respectively, the mouse was excluded from analysis.

Y maze spontaneous alternation test

Spontaneous alternation in Y maze was tested 24 h after new object recognition test. The Y maze has three arms separated from each other at the same angle (120°), and each arm was 30 cm long, 12 cm height, and 5 cm wide. Each mouse was placed at the intersection point of three arms and allowed to move freely for 8 min. The entries of mouse into each arm were recorded and every entry different from last two entries was considered as a successful alternation. The alternation percentage, an index of spatial working memory, was calculated according to the following: (number of alternations) / (total number of arm entries − 2) × 100%.

Morris water maze test

After Y maze test, the mice were subjected to Morris water maze (MWM) test to evaluate the long term spatial memory of mice. The maze was a circular pool with a diameter of 120 cm and a wall height of 50 cm. The pool was filled with water at a temperature of 23 ± 2 °C, and the water was made opaque with non-toxic white tempera paint. Various prominent visual cues were positioned on the inner wall of the pool. A platform (diameter, 12 cm; height, 29 cm) was submerged approximately 1.0 cm below the water surface at the midpoint of one quadrant of the pool. The swimming activity of each mouse was monitored via a camera mounted overhead, and a video tracking system (Ethovision 3.0, Noldus Information Technology, Wageningen, The Netherlands) was used to collect movement information (latency, swim path, distance and speed) of mice. In the hidden platform test, each mouse was trained four times per day for 5 consecutive days. On each experimental day, a trial was initiated by placing each mouse in the water facing the pool wall in one of the four quadrants and allowing it to swim freely to the escape platform. When mouse found the platform, it was allowed to stay on it for 5 s. If it did not find the platform within 60 s, the mouse was guided gently to the platform. And then the mouse was placed back to the home cage for 20 s before the next trail. On the next day after the hidden platform tests, each animal was given a 60 s probe trial to evaluate its memory retention ability. During the probe test, the platform was removed and the searching behavior of mice in the target quadrant (where the platform was located during hidden training) was measured.

In vivo hippocampal L-LTP recording

After behavioral tests, in vivo hippocampal L-LTP recording was performed. Mice were anesthetized with 5% chloral hydrate (0.07 ml/10 g, i.p.) and placed in a stereotaxic device for acute surgery and L-LTP recording. A bound stimulating/recording electrode was inserted into the CA1 region of hippocampus, with a tip location of the recording electrode at 2.0 mm posterior to the bregma and 1.5 mm lateral to the midline. Baseline field excitatory postsynaptic potentials (fEPSPs) were monitored for 30 min with repeated test stimuli (intensity, 30–50% of maximal EPSPs; frequency, 0.033 Hz) delivered to the Schaffer-collateral/commissural pathway. High-frequency stimulation (HFS) was applied to induce L-LTP of fEPSPs. The HFS consisted of 3 series stimuli with a 5 min interval, each series containing 3 trains of 20 stimuli with an inter-stimulus interval of 5 ms (200 Hz) and an inter-train interval of 30 s, as described in our previous studies [3, 4]. After 3 series of HFS, fEPSPs were evoked at 0.033 Hz for at least 3 h. The slop of fEPSP was normalized to basal fEPSP and averaged. To test whether presynaptic mechanism was involved, paired-pulse facilitation (PPF), a short-term enhancement of synaptic transmission, was also observed in the CA1 region by using paired stimuli with an interval of 50 ms before HFS. The change in the PPF ratio (calculated by dividing the slope of the second fEPSP by the slope of the first fEPSP) reflects the alteration of neurotransmitter release from presynaptic terminals.

Immunohistochemistry and immunofluorescence double labeling

After completion of LTP recording, the mice (n = 6 in each group) were sacrificed by heart perfusion fixation with phosphate-buffered saline (PBS) and 4% paraformaldehyde (PFA). The brains of the mice were rapidly dissected and post-fixed for 24 h at room temperature. Then the brains of the mice were

dehydrated. The brain blocks were sliced into 25-μm-thick coronal sections. For immunohistochemical staining, the sections were incubated in 5% H_2O_2 at room temperature for 15 min, followed by washing 3 times with 0.01 M PBS. After blocking in 5% goat serum (Solarbio, China) for 30 min, brain slices were incubated with primary antibodies [anti-Aβ antibody (6E10), dilution 1:500, 803105, Biolegend,USA; anti-GFAP antibody, dilution 1:200, bs-0199R, Bioss, China] overnight at 4 °C, and secondary antibodies (Biotin-goat anti-mouse IgG, dilution 1:100, BST10G22C01, Boster, China; Biotin-goat anti-rabbit IgG, dilution 1:100, BST10G22C03，Boster, China) were incubated at room temperature for 2 h after washing the primary antibodies with PBS three times. Then, the brain slices were incubated with ABC complex (1:200) and DAB method was applied for positive coloration. Images were analyzed with Image-Pro Plus 6.0 (Media Cybernetics, USA). For immunofluorescent staining, the sections were washed and blocked with 5% serum for 30 min. Then brain slices were incubated with primary antibodies [Anti-GFAP antibody, dilution 1:200, bs-0199R, Bioss, China] overnight at 4 °C, and secondary antibodies [GFAP: Alexa Fluor547-Donkey Anti-Rabbit IgG (H + L), 1:200，117995，Jackson，USA] for 2 h at room temperature in the dark. Then, the slices were incubated with the second primary antibodies [IL-1β Antibody (M-20): sc-1251，Santa，USA] overnight at 4 °C. The sections were incubated with Alexa Fluor488-conjugated Affinipure Bovine Anti-Goat IgG (H + L)(1:100,116969，Jackson，USA). The sections were incubated with DAPI for 10 min at room temperature. A laser scanning confocal microscope was used to obtain immunofluorescence images in the brain slices.

Western blot

One side of the mice hippocampi (n = 6 in each group) was dissected and used for measuring protein expression by western blot. The hippocampus was homogenized in tissue protein extraction reagent (Boster, Inc. China), supplemented with complete protease and phosphatase inhibitor (Boster, Inc. China). The homogenates were centrifuged (30 min, 15,000 rpm, 4 °C), and protein concentration was measured using BCA protein assay kit (Boster, Inc. China). A total of 50 μg of protein from each sample was used. Sample proteins were separated on 12% SDS-polyacrylamide gels. After electrophoresis, the proteins were transferred onto 0.45 μm PVDF membranes (Solarbio, inc. China) and nonspecific binding was blocked with 5% BSA (Solarbio, inc. China) in Tris-buffered saline containing 0.05% Tween-20 (TBST). The membranes were incubated with a primary antibody overnight at 4°C, followed by a secondary antibody for 2 h at 4°C. The primary antibodies used were as follows: Anti-Phospho-NF-κBp65 (Ser468) antibody (#3039,Cell Signaling Technology，USA, dilution 1:1000); Anti-NF-κBp65 antibody (#3034，Cell Signaling Technology，USA, dilution 1:1000);Anti-Phospho-PKA R2/PKR2 (phospho S99) antibody (ab32390, Abcam，UK, dilution 1:1000); Anti-PKA R2/PKR2 antibody (ab38949, Abcam，UK, dilution 1: 3000)，Anti-cAMP protein kinase catalytic subunit antibody (ab26322, Abcam，UK, dilution 1:1000); Anti-phosphor-CREB (phospho S133) antibody (ab32096，Abcam，UK, dilution 1:500); Anti-CREB antibody (ab31387, Abcam, UK, dilution 1:700), The secondary antibodies used were Biotin-goat anti-rabbit IgG (BST10G22C03，Boster, Inc. China, dilution 1:1000); Goat anti-rabbit IgG HRP (ZSGB-BIO, Inc. China, dilution1:100,000). After rinsing with TBST, the immunocomplexes were visualized by chemiluminescence using the ECL (Beyotime, Inc.). The film signals were digitally scanned with a Fluor Chem Scanner (Protein Simple) and quantified with Alpha View SA software. β-actin (PR-0255 ZSGB-BIO

Inc. China, dilution 1:3000) was utilized as an internal control for sample loading, and each blot was normalized to its corresponding β-actin value.

ELISA

The other side of the mice hippocampi (n = 6 in each group) were dissected and used to detect the content of IL-1β by Enzyme-linked immunosorbent assay (ELISA, SEA563Mu, Cloud-Clone Corp, USA). The hippocampal tissues were minced to small pieces and homogenized in fresh lysis buffer with a glass homogenizer on ice. The resulting suspension was sonicated with an ultrasonic cell disrupter till the solution is clarified. Then, the homogenates were centrifuged for 5 minutes at 10000 g. The supernatant was collected for analysis. At the same time, mouse plasma was collected for analysis of insulin level with another ELISA kit (CEA448Mu, Cloud-Clone Corp, USA). 5 wells were for standard points, 1 well for blank, and 3 replicate wells were set for each concentration standard. 50 μl detection reagent A was added to each well. The enzyme labeling plate was covered with a plate sealer and incubated for 1 hour at 37℃. After discarding the liquid in the well, 100 μl of the test solution B was added to each well for a 30 minutes of incubation at 37℃. Then, 90 μl of TMB substrate solution was added to each well. After 10–20 min of incubation, 50 μl of stop solution was added, and the optical density (OD value) of each well was measured at 450 nm wavelength.

Statistical analysis

All values are expressed as means ± standard errors (SEM). Mouse body weight, blood glucose, plasma insulin and water maze navigation data were analyzed using three-way repeated measures analysis of variance (ANOVA). Other data were analyzed using two-way repeated measures ANOVA and post hoc Tukey's test. Statistical significance was defined as $p < 0.05$, and all statistical analyses were performed using software packages SPSS 18.0 and SigmaPlot 12.0.

Results

DAla2GIP-Glu-PAL treatment enhanced new object recognition ability in APP/PS1 mice

Before new object recognition test, the motor capability of mice was evaluated in the open field task. As shown in Fig. 1A, there was no significant difference in total moving distance among the four groups (APP/PS1: $F_{(1,47)} = 3.532$, $P = 0.067$; DAla2GIP-Glu-PAL: $F_{(1,47)} = 0.204$, P = 0.655; APP/PS1 × DAla2GIP–Glu-PAL interaction: $F_{(1,47)} = 1.813$, $P = 0.189$). Thus, no evidence showed that APP/PS1 gene mutation and DAla2GIP-Glu-PAL treatment affect the motor capability of the mice. Based on the instinct of mice to explore new things, new object recognition test was performed on the second day after the open field test. Two-way ANOVA showed that APP/PS1 gene mutation and GIP analogs treatment had significant main effects on new object recognition memory (APP/PS1: $F_{(1,47)} = 23.507$, $P < 0.001$; DAla2GIP-Glu-PAL: $F_{(1,47)} = 4.626$, $P = 0.037$; APP/PS1 × DAla2GIP-Glu-PAL interaction: $F_{(1,47)} = 13.758$, $P < 0.001$). Tukey's *post hoc*

tests (Fig. 1B) showed that the RI in the APP/PS1 + PBS mice (49.12 ± 0.05%) significantly lower than that in the WT + PBS group (61.99 ± 0.04%, $P < 0.001$), indicating that the APP/PS1 mice spent less time in exploring the novel object. However, the RI in the APP/PS1 + DAla2GIP-Glu-PAL group (58.45 ± 0.03%) had a significant increase compared with the APP/PS1 + PBS mice ($P < 0.001$).

DAla2GIP-Glu-PAL alleviated working memory deficits in APP/PS1 mice

The spontaneous alternation of mice in Y maze was tested to examine the working memory of animals. Two-way ANOVA showed that APP/PS1 gene mutation and DAla2GIP-Glu-PAL treatment had significant main effects on the spontaneous alternation of the mice(APP/PS1: $F_{(1, 47)} = 7.223$,$P = 0.01$; DAla2GIP-Glu-PAL: $F_{(1, 47)} = 11.910$, $P < 0.01$; APP/PS1 × DAla2GIP-Glu-PAL interaction: ($F_{(1, 47)} = 4.626$, $P = 0.037$). Tukey's *post hoc* tests showed that the percentage of correct alternation in APP/PS1 + PBS (50.93 ± 1.97%) was significantly lower than that in WT + PBS group (61.51 ± 2.20%, $P < 0.01$). After treatment with DAla2GIP-Glu-PAL, the correct alternation percentage in APP/PS1 + DAla2GIP-Glu-PAL group (63.30 ± 2.64%) had a significant increase ($P < 0.01$) compared with APP/PS1 + PBS mice (Fig. 2A). Meantime, the total arm entries of mice did not show any significant difference among these groups ($P > 0.05$, Fig. 2B), suggesting that the differences in spontaneous alternation among groups were due to impairment of spatial working memory rather than a disability of locomotor activity.

DAla2GIP-Glu-PAL improved long term spatial learning and memory of APP/PS1 mice

The MWM was used to assess the long term spatial learning and memory of mice. The learning ability of mice to acquire spatial information was first assessed by a consecutive 5 days of hidden platform test. As shown in the table 1 and Fig. 3A, the escape latency in all groups gradually decreased with the increase of training days. Although there was no significant difference among groups on day 1 and day 2, the mean escape latency had a significant increase in the APP/PS1 + PBS group on days 3–5, compared with the WT + PBS group. Interestingly, the increased escape latency was significantly decreased in the APP/PS1 + DAla2GIP-Glu-PAL group on days 4–5. This result indicates that chronic DAla2GIP-Glu-PAL treatment could improve the spatial learning ability of APP/PS1 mice.

Table.1 Mean escape latencies of mice during 5 training days (s, Mean ± S.E.M.)

Group (n =12 in each group)	Day 1	Day 2	Day 3	Day 4	Day 5
WT+PBS	54.22±2.44	52.27±4.35	30.77±4.06	33.08±3.63	21.69±4.28
APP/PS1+PBS	56.71±1.94	55.52±1.90	54.60±2.39**	46.08±3.73**	44.62±3.89**
WT+DAla2GIP-Glu-PAL	52.26±2.18	43.33±3.06	36.16±4.15	28.45±4.69	29.59±4.51
APP/PS1+DAla2GIP-Glu-PAL	55.94±1.88	49.22±3.68	42.50±5.16	35.07±3.85##	29.47±4.93##

**P < 0.01 vs. WT+PBS group; ## P <0.01 vs. APP/PS1+PBS group.

To exclude the possibility that the difference in escape latency might be caused by drug-induced visual and locomotor deficits, a visual platform test was performed after the probe trials. Statistical analysis showed that there was no significant difference in the swimming speed in probe trials and the swimming time arriving the visible platform between groups (Fig. 3D and E, P > 0.05), suggesting that the changes in escape latency and swimming time percentage exactly resulted from the impairments of spatial learning and memory.

DAla2GIP-Glu-PAL reversed in vivo hippocampal L-LTP suppression in APP/PS1 mice

To clarify the possible mechanism underlying the neuroprotective effects of DAla2GIP-Glu-PAL on learning and memory, we investigated the effects of DAla2GIP-Glu-PAL on the long term synaptic plasticity by recording *in vivo* fEPSPs in the hippocampal CA1 region. After 30 min of stable basal fEPSP recording, three series of HFS were given to induce L-LTP. The potentiation of fEPSPs was compared at 60 min, 120 min, and 180 min after HFS (Fig. 4). Two-way ANOVA demonstrated that APP/PS1 gene mutation and DAla2GIP-Glu-PAL treatment had significant main effects on the fEPSP slope at 60 min (APP/PS1: $F_{(1,26)}$ = 3.321, P = 0.028; DAla2GIP-Glu-PAL: $F_{(1,26)}$ = 4.380, P = 0.005; APP/PS1 × DAla2GIP-Glu-PAL interaction: $F_{(1,26)}$ = 4.917, P = 0.002), 120 min (APP/PS1: $F_{(1,26)}$ = 4.799, P = 0.003; DAla2GIP-Glu-PAL: $F_{(1,26)}$ = 4.215, P = 0.007; APP/PS1DAla2GIP-Glu-PAL interaction: $F_{(1,26)}$ = 6.096, P < 0.001) and 180 min (APP/PS1: $F_{(1,26)}$ = 6.802, P < 0.001; DAla2GIP-Glu-PAL: $F_{(1,26)}$ = 4.425, P = 0.005; APP/PS1 × DAla2GIP-Glu-PAL interaction: $F_{(1,26)}$ = 8.546, P < 0.001) post-HFS. Tukey's *post hoc test* shown that the slopes of the fEPSPs immediately after HFS abruptly increased from 100% to 219.5 ± 1.16%, 202.34 ± 4.39%, 220.93 ± 2.74%, and 220.32 ± 4.19% in the WT + PBS, APP/PS1 + PBS, WT + DAla2GIP-Glu-PAL, and APP/PS1 + Dala2GIP-Glu-PAL groups, respectively, indicating that LTP was successfully induced in the four groups (Fig. 4A). However, the L-LTP values in the APP/PS1-PBS group obviously decreased from 40 min post-HFS. As shown in the Fig. 4A and 4C, compared with the WT + PBS mice, the L-LTP value was significantly suppressed at 60 min (131.92 ± 8.57%, P < 0.05), 120 min (121.76 ± 6.36%, P < 0.05) and 180 min (103.57 ± 1.67%, P < 0.05) in APP/PS1 + PBS mice. In contrast, there was a relative large

maintenance of L-LTP in the APP/PS1 + DAla2GIP-Glu-PAL group at 60 min (177.28 ± 5.97%, $P < 0.05$), 120 min (165.58 ± 6.06%, $P < 0.05$) and 180 min (162.41 ± 7.08%, $P < 0.05$) compared with the APP/PS1 + PBS group.

Further, paired pulse facilitation (PPF) was examined to detect the possible involvement of presynaptic mechanism in the effects of DAla2GIP-Glu-PAL on the LTP (Fig. 4D). Application of paired pulses to the Schaffer collaterals always induced PPF (see inset of Fig. 4D). Two way ANOVA showed that APP/PS1 gene mutation and DAla2GIP-Glu-PAL treatment had no significant main effects on PPF (APP/PS1: $F_{(1,26)} = 0.369$, $P = 0.550$; DAla2GIP-Glu-PAL: $F_{(1,26)} = 0.003$, $P = 0.956$; APP/PS1 × DAla2GIP-Glu-PAL interaction: $F_{(1,26)} = 0.298$, $P = 0.590$). Thus, no evidence showed that APP/PS1 gene mutation and DAla2GIP-Glu-PAL treatment affected presynaptic neurotransmitter release in the hippocampal CA1 region.

DAla2GIP-Glu-PAL treatment reduced Aβ plaques in the hippocampus of APP/PS1 mice

High-density Aβ plaques is typical pathological hallmarks in the AD brains. In the immunohistochemistry, we aimed to evaluate the histopathological changes in the hippocampus of mice. Aβ plaques were detected using specific antibodies 6E10 (Fig. 5). Two way ANOVA showed that APP/PS1 gene mutation and DAla2GIP-Glu-PAL treatment had significant main effects on the numbers of 6E10 positive plaques (APP/PS1: $F_{(1,23)} = 222.732$, $P < 0.001$; DAla2GIP-Glu-PAL: $F_{(1,23)} = 52.745$, $P < 0.001$;APP/PS1 × DAla2GIP-Glu-PAL interaction: $F_{(1,23)} = 52.745$,$P < 0.001$). As shown in the Fig. 5A, 6E10 positive plaques could be easily seen in the hippocampus of APP/PS1 transgenic mice under low magnification. Tukey's *post hoc* test showed that the number of Aβ plaques in APP/PS1 + PBS group (15.13 ± 0.89) was significantly more than that in WT + PBS group (0.33 ± 0.00, $P < 0.001$), while DAla2GIP-Glu-PAL treatment effectively reduced the number in the hippocampus of APP/PS1 mice (6.98 ± 0.46, $P < 0.001$). These results above demonstrated that DAla2GIP-Glu-PAL treatment could attenuate cerebral pathological changes in the APP/PS1 transgenic mice.

DAla2GIP-Glu-PAL attenuated inflammatory response in the hippocampus of APP/PS1 transgenic mice

In view of the fact that Aβ can promote astrocyte proliferation and trigger inflammatory reactions in the brain, we further observed the effects of DAla2GIP-Glu-PAL injection on the inflammatory responses in the APP/PS1 transgenic mice by using immunohistochemistry and immunofluorescence double labeling techniques (Fig. 6). Two way ANOVA showed that APP/PS1 gene mutation and DAla2GIP-Glu-PAL treatment had significant main effects on intensity of GFAP, astrocyte specific antibody (APP/PS1: $F_{(1,23)} = 43.197$,$P < 0.001$; DAla2GIP-Glu-PAL: $F_{(1,23)} = 13.259$, $P = 0.002$;APP/PS1 × DAla2GIP-Glu-PAL interaction: $F_{(1,23)} = 8.459$ $P = 0.009$). As shown in the Fig. 6A and C, Tukey's *post hoc* test showed that the GFAP

immunoreactivity had a significant increase in the APP/PS1 + PBS group (163.38 ± 12.21%) compared with the WT + PBS group (100.24 ± 4.71%) ($P < 0.001$), while the increased GFAP value has a significant reduction in DAla2GIP-Glu-PAL treated APP/PS1 group (120.14 ± 3.23%) ($P < 0.001$).

Because Aβ and phosphorylated Tau can stimulate astrocytes to synthesize and secrete inflammatory factors such as IL-1β, we further observed the double staining of GFAP-positive astrocytes and inflammatory factor IL-1β by immunofluorescence technique. As shown in the Fig. 6B, there were small number of GFAP (red) and IL-1β (green) immunopositive cells in the hippocampus of the WT + PBS and WT + DAla2GIP-Glu-PAL groups, while a lot of GFAP and IL-1β positive cells were found in the APP/PS1 + PBS group. The increased GFAP and IL-1β positive cells were significantly reduced after treatment with DAla2GIP-Glu-PAL. We further tested the content of IL-1β in the hippocampus by ELISA. Two way ANOVA showed that APP/PS1 gene mutation and DAla2GIP-Glu-PAL treatment had significant main effects and interaction on IL-1β content (APP/PS1: $F_{(1,23)} = 145.079$, $P < 0.001$; DAla2GIP-Glu-PAL: $F_{(1,23)} = 49.654$, $P < 0.001$;APP/PS1 × DAla2GIP-Glu-PAL interaction $F_{(1,23)} = 34.968$, $P < 0.001$). Tukey's *post hoc* test showed that IL-1β OD values was significantly increased in the APP/PS1 + PBS group (331.61%±16.37%) compared with the WT + PBS group (126.77%±8.19%, $P < 0.001$), while treatment with DAla2GIP-Glu-PAL significantly reduced the values of IL-1β in the APP/PS1 + DAla2GIP-Glu-PAL group (183.78%±11.63%, $P < 0.001$, Fig. 6D).

In addition, considering that IL-1β and TNF-α can activate NF-κB to enter the nucleus and up-regulate the expression of inflammatory factors, and trigger the inflammatory cells proliferation [28, 29], we also examined the expression level of NF-κBp65 (Ser468) in the hippocampus by western blot (Fig. 6E and F). Two way ANOVA showed that APP/PS1 gene mutation and DAla2GIP-Glu-PAL treatment had significant main effects and interaction on NF-κBp65 (Ser468) expression level (APP/PS1: $F_{(1,23)} = 19.269$, $P < 0.001$; DAla2GIP-Glu-PAL: $F_{(1,23)} = 14.293$, $P < 0.001$;APP/PS1 × DAla2GIP-Glu-PAL interaction $F_{(1,23)} = 4.964$, $P = 0.038$). Tukey's *post hoc* test showed that the value of NF-κBp65 (Ser468) in the hippocampus of APP/PS1 + PBS mice (141.95%±8.31%) was significantly higher than that of other groups ($P < 0.01$), while DAla2GIP-Glu-PAL significantly reduced the expression level of NF-κBp65 in APP/PS1 + DAla2GIP-Glu-PAL group (103.86%±5.94%, $P < 0.01$). These results indicate that chronic i.p. injection of DAla2GIP-Glu-PAL attenuated inflammatory response in the hippocampus of APP/PS1 mice.

The DAla2GIP-Glu-PAL treatment up-regulated the expression levels of cAMP, ^{S99}p-PKA and ^{S133}p-CREB in the hippocampus of APP/PS1 transgenic mice

To investigate the possible mechanism of DAla2GIP-Glu-PAL in improving cognitive behavior and pathological features of APP/PS1 transgenic mice, we detected the expression levels of cAMP, ^{S99}p-PKA and ^{S133}p-CREB in the hippocampus. As shown in the Table 2, the two way ANOVA showed that the APP/PS1 gene mutation and DAla2GIP -Glu-PAL drug treatment have obvious main effects and

interaction effects on each signal molecule. The typical Western-blotting bands and Tukey's *post hoc* test (Fig. 7) showed that the relative gray values of cAMP, ^{S99}p-PKA, ^{S133}p-CREB were significantly decreased ($P < 0.01$) in APP/PS1 + PBS group compared with that in WT + PBS group. However, chronic i.p. injection of DAla2GIP-Glu-PAL effectively reversed the down-reglulation ($P < 0.01$). These results indicate that neuroprotective effects of DAla2GIP-Glu-PAL may be involved in the up-regulation of cAMP/ PKA/ CREB signaling pathway in the hippocampus of APP/PS1-PBS mice.

Table.2 Two-way ANOVA for the levels of cAMP, ^{S99}p-PKA and ^{S133}p-CREB in the hippocampus. (n=6 in each group)

Protein	Main effect		Interaction effect
	APP/PS1	DAla2GIP-Glu-PAL	
cAMP	38.243，P<0.001，	28.028，P<0.001，	11.052，P=0.003，
^{S99}p-PKA	21.237，P<0.001，	11.584，P=0.003，	4.558，P=0.045，
^{S133}p-CREB	32.412，P<0.001，	20.127，P<0.001，	8.669，P=0.008，

Discussion

Working memory and spatial reference memory are dependent on hippocampal functions[3]. Therefore, the memory disorder will gradually aggravate with the development of hippocampal dysfunction during AD processes. Although the exact pathogenesis of AD remains elusive, mutations of several genes such as amyloid-β precursor protein (APP), presenilin-1 (PS1) and presenilin-2 (PS2) has been closely linked to AD[29]. Moreover, the APP/PS1 mice with memory impairments and hippocampal pathology have been widely used in the AD research [30, 31]. In the present study, 9-month-old APP/PS1 mice were first subjected to multiple behavioral tests. The decreased RI in new object recognition test and reduced spontaneous alternation in Y maze clearly indicate impairment in short-term memory in the APP/PS1 mice, while the increased escape latency in place navigation and decreased swimming time in probe test in MWM suggest an obvious decline in spatial long-term learning and memory in APP/PS1 mice. These results are consistent with previous reports for the APP/PS1 mouse model of AD[18, 32, 33]. Importantly, we found for the first time that intraperitoneal injection of DAla2GIP-Glu-PAL effectively alleviates the cognitive deficits in the APP/PS1 transgenic mice, with significant improvements in working memory and long-term reference memory. These behavioral experiments suggest that DAla2GIP-Glu-PAL treatment may be an effective strategy for the cognitive decline in AD.

Due to a close association between spatial memory and hippocampal synaptic plasticity, hippocampal LTP has been deemed to be a major cellular mechanism underlying learning and memory[34, 35]. Previously, we have demonstrated that intracerebroventricular (i.c.v.) injection of Aβ1−42 suppressed in vivo hippocampal L-LTP in normal rats[3]. In the present study, we confirmed that the in vivo L-LTP in the hippocampal CA1 region was also seriously impaired in the APP/PS1 double transgenic mice. The L-LTP value was significantly suppressed at 60 min, 120 min and 180 min in APP/PS1 mice. Unlike the early phase LTP (E-LTP), the L-LTP requires new protein synthesis and correlates much with the long-term memory. Of particular note is the L-LTP recordings in the present study were conducted on the same behaviorally trained mice, which thus providing further insights on the relationship between the spatial memory and hippocampal L-LTP in the APP/PS1 mice. Interestingly, DAla2GIP-Glu-PAL treatment improved hippocampal synaptic plasticity in the transgenic mice, with relative larger and longer

maintenance of L-LTP in the APP/PS1 + DAla2GIP-Glu-PAL group. Therefore, the electrophysiological results of L-LTP support the behavioral improvement induced by DAla2GIP-Glu-PAL in the APP/PS1 mice.

Aβ is a main pathological biomarker in the AD brain, which triggers synaptic dysfunction, neuronal degeneration, astrocyte proliferation and cognitive disorders in rats and mice [36–39]. Astrocytes are also capable of synthesizing and secreting cytokines, including TNF-α, IL-1β, IL-6 and TGF-β. Impairments in astrocytes can trigger or exacerbate hyperphosphorylated tau and Aβ pathologies, leading to the formation of both amyloid plaques and neurofbrillary tangles (NFTs), as well as neuronal dysfunction. Our recent study also justified that not only microglia but also astrocytes in the hippocampus of AD mice displayed stronger activation[40]. More importantly, a kind of GLP1 analog liraglutide has shown a beneficial effect in the hippocampal inflammation including reactive microgliosis and astrogliosis[41]. Therefore, the present study further explored the neuroinflammatory responses caused by astrocytes and the effects of DAla2-GIP-glu-PAL on the inflammatory response in APP/PS1 transgenic mice. Interestingly, the present study found that large number of Aβ plaques and astrocyte proliferation appeared in the hippocampus of 9-month-old APP/PS1 mice, while DAla2GIP-Glu-PAL treatment attenuated the cerebral pathological change. Further, the immunofluorescence double labeling well demonstrated the coexistence of GFAP and IL-1β in the hippocampus of APP/PS1 transgenic mice. ELISA and western blot results showed that the contents of IL-1β and phosphorylated NF-κBp65 in the brain of APP/PS transgenic mice were significantly increased. These results indicate that IL-1β and NF-κBp65 induced inflammatory damage may be closely associated with Aβ deposition in the brain of APP/PS1 transgenic mice. As we know, NF-κB is widely expressed in human tissue cells and is involved in cell proliferation, differentiation, apoptosis, and inflammation. When cells are stimulated by appropriate extracellular substances such as proinflammatory cytokines and neurotoxic Aβ, NF- κB can be activated and enters the nucleus to regulate gene expression of various proteins [42]. Studies have confirmed that inflammatory factors such as TNF-α and IL-1β can activate NF-κB, which in turn not only up-regulates inflammatory factors and triggers inflammatory cell proliferation such as astrocytes[43, 44], but also up-regulates the expression of β-secretase and APP genes, and promotes the production of Aβ[45]. So, the mutual dependence and mutual promotion between inflammatory response and pathological Aβ in the brain would accelerate the progression of AD. On one hand, the Aβ deposition induces astrocyte proliferation, which promotes the synthesis and secretion of inflammatory factors, thereby activates nuclear transcriptional effects of NF-κB, and aggravates inflammatory reaction in the brain. On the other hand, the proliferation of astrocytes and activation of NF-κB can inhibit the phagocytic and scavenging effects of microglia on senile plaques, and increase the deposition of senile plaques by inhibiting Aβ autophagy, aggravating pathological damage and inflammation in the brain[46]. It is interesting that DAla2GIP-Glu-PAL chronic treatment in the present study broke the vicious circle and effectively reduced Aβ plaque and inflammatory response in the hippocampus of APP/PS1 transgenic mice.

It is reported that GIP, as an incretin growth factor, activates pancreatic islets to enhance insulin secretion and has a signaling pathway parallel to insulin. However, the present study found that DAla2GIP-Glu-PAL treatment for more than 28 days did not affect the plasma insulin, as well as the body weight and blood glucose in AD or WT mice (data not shown). Similarly, our recently published data [38] also show that i.p.

injection of another novel candidate drug for treating T2DM did not affect the plasma insulin, body weight and blood glucose of APP/PS1/Tau transgenic mice. Therefore, we speculate that the neuroprotective effects of DAla2GIP-Glu-PAL by i.p. injection are mediated by GIP receptors in the brain. The GIP receptor (GIPR) is a member of G-protein-coupled receptor superfamily. It has been justified that GIPR KO mice had clear impairments in memory formation, synaptic plasticity, and progenitor cell proliferation[47]. GIP(3–30)NH2, a competitive antagonist of GIPR, effectively inhibited GIP-mediated insulin, glucagon, and somatostatin release[48]. The GIP's effect on bone metabolism was also reduced by the selective GIPR antagonist GIP(3–30)NH_2[49]. Activation of GIPRs by native GIP or protease-resistant analogs, such as Nacetyl-GIP, enhanced synaptic plasticity and protected synapses from the detrimental effects of Aβ on LTP formation, however, the selective GIP antagonist Pro(3)GIP weakened the synaptic plasticity[22]. These findings clearly demonstrate that the GIPR plays an important role in neuronal communication and brain function. Activation of GIP receptors is coupled to increases in cAMP and intracellular Ca^{2+} levels, as well as activation of PI3K, PKA and PKB. Our study also showed that the levels of cAMP/p-PKA/p-CREB in the hippocampus of APP/PS1 mice were significantly decreased, while chronic intraperitoneal injection of DAla2GIP-Glu-PAL effectively reversed the decline in these signal molecules. These results indicate that DAla2GIP-Glu-PAL, by up-regulating cAMP/p-PKA/p-CREB signal pathway, can improve cognitive function and synaptic plasticity, and ameliorate pathological damage and inflammatory injury in the hippocampus of APP/PS1 mice. Li et al. also reported that DAla2GIP-Glu-PAL reduced damage of dopaminergic neurons and neuroinflammation in Parkinson's disease mouse model by increasing CREB and Bcl-2 expression in the brain[28]. In addition, up-regulation of PI3K/AKT1 and down-regulation of GSK3β in the hippocampus of APP/PS1 transgenic mouse might be also linked to the neuroprotection of DAla2GIP-Glu-PAL[50].

Conclusions

The present study demonstrated for the first time that chronic application of DAla2GIP-Glu-PAL could effectively improve multiple cognitive behaviors of APP/PS1 mice and reduce AD-like pathological damages in the brain. DAla2GIP-Glu-PAL significantly inhibited astrocyte proliferation and IL-1β secretion. DAla2GIP-Glu-PAL also up-regulate cAMP/PKA/CREB signal transduction and inhibited NF-κB activation in the hippocampus of APP/PS1 mice. These results indicate that DAla2GIP-Glu-PAL can prevent cognitive deficits and pathological damage of APP/PS1 mice by reducing neuroinflammation and improving synaptic plasticity, suggesting that DAla2GIP-Glu-PAL might be potentially beneficial in the treatment of AD.

Abbreviations

Aβ: amyloid-β; AD: Alzhermer's disease; APP: amyloid-β precursor protein; APP/PS1: APP_{swe}/$PS1_{dE9}$; BBB: blood brain barrier; cAMP: cyclic adenosine monophosphate; CREB: cAMP response element binding protein; DPP-IV: the enzyme dipeptidyl peptidase IV; fEPSPs: field excitatory postsynaptic potentials; GFAP: Glial fibrillary acidic protein; GIP: Glucose-dependent insulinotropic polypeptide; GSK-3β: Glycogen

synthase kinase 3 beta; IL-1β: Interleukin 1 beta; i.p.: intraperitoneal injection; L-LTP: late-phase long-term potentiation; MWM: Morris water maze; NFTs: neurofibrillary tangles; NF-κBp65: Nuclear transcription factor-kappa Bp65; PKA: protein kinase A; PPF: paired pulse facilitation; PS1: presenilin-1; PS2: presenilin-2; TNF-α: Tumor necrosis factor-alpha; T2DM: Type 2 diabetes mellitus

Declarations

Ethics approval and consent to participate

The experiments were approved by the Institute of Laboratory Animal Sciences in Beijing (SCXX: 2013-0002) and by the Shanxi Committee on Ethics of Animal Research.

Consent for publication

Not applicable.

Availability of data and materials

The data that support the findings are not publicly available. Data are available from the authors upon reasonable request.

Competing interests

The authors declare that they have no competing interests.

Funding

This research was supported by the following programs: National Natural Science Foundation of China (31471080, 31700918, 31600865 and 81600951); Fund Program for “Sanjin Scholars” of Shanxi Province, Shanxi Province Science Foundation for Excellent Young Scholars (No.201801D211005) Alzheimer Society and Alzheimer Drug Discovery Foundation (124660); Fund for Shanxi Key Subjects Construction, FSKSC, Shanxi “1331 Project” Key Subjects Construction (1331KSC) and Key Laboratory of Cellular Physiology (Shanxi Medical University) in Shanxi Province; Scientific and technological Innovation Project of Colleges and Universities in Shanxi Province (2017166); Changzhi Medical College Doctoral Initiation Fund (BS17001).

Authors’ contributions

JSQ, CH and LY conceived the idea. LY analyzed most experiments and wrote the manuscript. JSQ revised the manuscript. JZ and JTY performed the immunohistochemistry and immunofluorescence double labeling. HS did the L-LTP surgery and recorded fEPSP. YFH and LNH bred the APP/PS1 mice and measured the IL-1β and NF-κBp65. MNW, ZJW and HYC collected the data. All authors read and approved the final manuscript.

Acknowledgments

We thank the staff at Department of Physiology, Key Laboratory of Cellular Physiology, Ministry of Education, Shanxi Medical University for providing experimental space and facilities.

Author details

[1]Department of Physiology, Changzhi Medical College, No.161 Jiefang East Street, Changzhi 046000, Shanxi, PR China

[2]Department of Physiology, Key Laboratory of Cellular Physiology, Ministry of Education, Shanxi Medical University, No.56 Xinjian South Road, Taiyuan 030001, Shanxi PR China

[3]Research and Experimental Center, Henan University of Chinese Medicine, No.156 Jinshui East Road, Zhengdong New Area, Zhengzhou 450046, Henan, PR China

[4]Department of Immunology and Microbiology, Shanxi Medical University, No.56 Xinjian South Road, Taiyuan 030001, Shanxi, PR China

References

1. Christina P, Paola B. World Alzheimer Report 2018 The state of the art of dementia research:New frontiers. Alzheimer Disease International. 2018;https://www.alz.co.uk/research/.
2. Citron M. Alzheimer's disease: strategies for disease modification. Nat Rev Drug Discov. 2010;9:387-98.
3. Tong JQ, Zhang J, Hao M, Yang J, Han YF, Liu XJ*, et al.* Leptin attenuates the detrimental effects of beta-amyloid on spatial memory and hippocampal later-phase long term potentiation in rats. Horm Behav. 2015;73:125-30.
4. Han WN, Holscher C, Yuan L, Yang W, Wang XH, Wu MN*, et al.* Liraglutide protects against amyloid-beta protein-induced impairment of spatial learning and memory in rats. Neurobiol Aging. 2013;34:576-88.
5. Wang ZJ, Han WN, Yang GZ, Yuan L, Liu XJ, Li QS*, et al.* The neuroprotection of Rattin against amyloid beta peptide in spatial memory and synaptic plasticity of rats. Hippocampus. 2014;24:44-53.
6. Wilkaniec A, Gassowska-Dobrowolska M, Strawski M, Adamczyk A, Czapski GA. Inhibition of cyclin-dependent kinase 5 affects early neuroinflammatory signalling in murine model of amyloid beta toxicity. J Neuroinflammation. 2018;15:1.
7. Y Z, Y D, JM G, C L, LH L, JS S*, et al.* Icariside II inhibits lipopolysaccharide-induced inflammation and amyloid production in rat astrocytes by regulating IKK/IκB/NF-κB/BACE1 signaling pathway. Acta pharmacologica Sinica. 2019;undefined:undefined.

8. Solana C, Tarazona R, Solana R. Immunosenescence of Natural Killer Cells, Inflammation, and Alzheimer's Disease. Int J Alzheimers Dis. 2018;2018:3128758.
9. Guan PP, Liang YY, Cao LL, Yu X, Wang P. Cyclooxygenase-2 Induced the beta-Amyloid Protein Deposition and Neuronal Apoptosis Via Upregulating the Synthesis of Prostaglandin E2 and 15-Deoxy-Delta(12,14)-prostaglandin J2. Neurotherapeutics. 2019.
10. Walker JM, Harrison FE. Shared Neuropathological Characteristics of Obesity, Type 2 Diabetes and Alzheimer's Disease: Impacts on Cognitive Decline. Nutrients. 2015;7:7332-57.
11. Mittal K, Katare DP. Shared links between type 2 diabetes mellitus and Alzheimer's disease: A review. Diabetes Metab Syndr. 2016;10:S144-9.
12. Ohara T. [Glucose tolerance status and risk of dementia in the community: the Hisayama study]. Seishin Shinkeigaku Zasshi. 2013;115:90-7.
13. Rosales-Corral S, Tan DX, Manchester L, Reiter RJ. Diabetes and Alzheimer disease, two overlapping pathologies with the same background: oxidative stress. Oxid Med Cell Longev. 2015;2015:985845.
14. Talbot K, Wang HY, Kazi H, Han LY, Bakshi KP, Stucky A*, et al.* Demonstrated brain insulin resistance in Alzheimer's disease patients is associated with IGF-1 resistance, IRS-1 dysregulation, and cognitive decline. J Clin Invest. 2012;122:1316-38.
15. Holscher C. Insulin, incretins and other growth factors as potential novel treatments for Alzheimer's and Parkinson's diseases. Biochem Soc Trans. 2014;42:593-9.
16. Claxton A, Baker LD, Hanson A, Trittschuh EH, Cholerton B, Morgan A*, et al.* Long-acting intranasal insulin detemir improves cognition for adults with mild cognitive impairment or early-stage Alzheimer's disease dementia. J Alzheimers Dis. 2015;44:897-906.
17. Moloney AM, Griffin RJ, Timmons S, O'Connor R, Ravid R, O'Neill C. Defects in IGF-1 receptor, insulin receptor and IRS-1/2 in Alzheimer's disease indicate possible resistance to IGF-1 and insulin signalling. Neurobiol Aging. 2010;31:224-43.
18. Faivre E, Holscher C. Neuroprotective effects of D-Ala(2)GIP on Alzheimer's disease biomarkers in an APP/PS1 mouse model. Alzheimers Res Ther. 2013;5:20.
19. K K. Incretin effect: GLP-1, GIP, DPP4. Diabetes research and clinical practice. 2011:S32-6.
20. Holscher C. Novel dual GLP-1/GIP receptor agonists show neuroprotective effects in Alzheimer's and Parkinson's disease models. Neuropharmacology. 2018;136:251-59.
21. Holscher C. Incretin analogues that have been developed to treat type 2 diabetes hold promise as a novel treatment strategy for Alzheimer's disease. Recent Pat CNS Drug Discov. 2010;5:109-17.
22. Gault VA, Holscher C. Protease-resistant glucose-dependent insulinotropic polypeptide agonists facilitate hippocampal LTP and reverse the impairment of LTP induced by beta-amyloid. J Neurophysiol. 2008;99:1590-5.
23. Figueiredo CP, Pamplona FA, Mazzuco TL, Aguiar AS, Jr., Walz R, Prediger RD. Role of the glucose-dependent insulinotropic polypeptide and its receptor in the central nervous system: therapeutic potential in neurological diseases. Behav Pharmacol. 2010;21:394-408.

24. Kieffer TJ, McIntosh CH, Pederson RA. Degradation of glucose-dependent insulinotropic polypeptide and truncated glucagon-like peptide 1 in vitro and in vivo by dipeptidyl peptidase IV. Endocrinology. 1995;136:3585-96.
25. Li Y, Liu W, Li L, Holscher C. Neuroprotective effects of a GIP analogue in the MPTP Parkinson's disease mouse model. Neuropharmacology. 2016;101:255-63.
26. Hunter K, Holscher C. Liraglutide, (dAla2)GIP and Ac-GIP Cross the Blood Brain Barrier. poster ARUK Conference, Leeds. 2011.
27. Faivre E, McClean P, Hölscher C. Novel GIP analogues cross the BBB and have effects on cognitive processes and synaptic plasticity in the hippocampus. . Paper presented at the Annual conference of the Alzheimer Research Trust UK, Southampton. 2010.
28. Li Y, Liu W, Li L, Holscher C. D-Ala2-GIP-glu-PAL is neuroprotective in a chronic Parkinson's disease mouse model and increases BNDF expression while reducing neuroinflammation and lipid peroxidation. Eur J Pharmacol. 2017;797:162-72.
29. Cacace R, Sleegers K, Van Broeckhoven C. Molecular genetics of early-onset Alzheimer's disease revisited. Alzheimers Dement. 2016;12:733-48.
30. Park JH, Ju YH, Choi JW, Song HJ, Jang BK, Woo J*, et al.* Newly developed reversible MAO-B inhibitor circumvents the shortcomings of irreversible inhibitors in Alzheimer's disease. Sci Adv. 2019;5:eaav0316.
31. Tabassum S, Misrani A, Tang BL, Chen J, Yang L, Long C. Jujuboside A prevents sleep loss-induced disturbance of hippocampal neuronal excitability and memory impairment in young APP/PS1 mice. Sci Rep. 2019;9:4512.
32. Webster SJ, Bachstetter AD, Nelson PT, Schmitt FA, Van Eldik LJ. Using mice to model Alzheimer's dementia: an overview of the clinical disease and the preclinical behavioral changes in 10 mouse models. Front Genet. 2014;5:88.
33. Webster SJ, Bachstetter AD, Van Eldik LJ. Comprehensive behavioral characterization of an APP/PS-1 double knock-in mouse model of Alzheimer's disease. Alzheimers Res Ther. 2013;5:28.
34. Shiosaka S, Ishikawa Y. Neuropsin–a possible modulator of synaptic plasticity. J Chem Neuroanat. 2011;42:24-9.
35. Qiao F, Gao XP, Yuan L, Cai HY, Qi JS. Apolipoprotein E4 impairs in vivo hippocampal long-term synaptic plasticity by reducing the phosphorylation of CaMKIIalpha and CREB. J Alzheimers Dis. 2014;41:1165-76.
36. Jo J, Whitcomb DJ, Olsen KM, Kerrigan TL, Lo SC, Bru-Mercier G*, et al.* Abeta(1-42) inhibition of LTP is mediated by a signaling pathway involving caspase-3, Akt1 and GSK-3beta. Nat Neurosci. 2011;14:545-7.
37. Yuan L, Liu XJ, Han WN, Li QS, Wang ZJ, Wu MN*, et al.* [Gly14]-Humanin Protects Against Amyloid beta Peptide-Induced Impairment of Spatial Learning and Memory in Rats. Neurosci Bull. 2016;32:374-82.

38. Li T, Jiao JJ, Holscher C, Wu MN, Zhang J, Tong JQ*, et al.* A novel GLP-1/GIP/Gcg triagonist reduces cognitive deficits and pathology in the 3xTg mouse model of Alzheimer's disease. Hippocampus. 2018;28:358-72.
39. Guillamon-Vivancos T, Gomez-Pinedo U, Matias-Guiu J. Astrocytes in neurodegenerative diseases (I): function and molecular description. Neurologia. 2015;30:119-29.
40. Yang JT, Wang ZJ, Cai HY, Yuan L, Hu MM, Wu MN*, et al.* Sex Differences in Neuropathology and Cognitive Behavior in APP/PS1/tau Triple-Transgenic Mouse Model of Alzheimer's Disease. Neurosci Bull. 2018;34:736-46.
41. ARC B-V, MB A, CA M-d-L. Beneficial effects of liraglutide (GLP1 analog) in the hippocampal inflammation. Metabolic brain disease. 2017;32:1735-45.
42. Chen CH, Zhou W, Liu S, Deng Y, Cai F, Tone M*, et al.* Increased NF-kappaB signalling up-regulates BACE1 expression and its therapeutic potential in Alzheimer's disease. Int J Neuropsychopharmacol. 2012;15:77-90.
43. Spilsbury A, Vauzour D, Spencer JP, Rattray M. Regulation of NF-kappaB activity in astrocytes: effects of flavonoids at dietary-relevant concentrations. Biochem Biophys Res Commun. 2012;418:578-83.
44. Dvoriantchikova G, Ivanov D. Tumor necrosis factor-alpha mediates activation of NF-kappaB and JNK signaling cascades in retinal ganglion cells and astrocytes in opposite ways. Eur J Neurosci. 2014;40:3171-8.
45. Chinchalongporn V, Shukla M, Govitrapong P. Melatonin ameliorates Abeta42 -induced alteration of betaAPP-processing secretases via the melatonin receptor through the Pin1/GSK3beta/NF-kappaB pathway in SH-SY5Y cells. J Pineal Res. 2018;64:e12470.
46. Ringman JM, Elashoff D, Geschwind DH, Welsh BT, Gylys KH, Lee C*, et al.* Plasma signaling proteins in persons at genetic risk for Alzheimer disease: influence of APOE genotype. Arch Neurol. 2012;69:757-64.
47. Faivre E, Gault VA, Thorens B, Holscher C. Glucose-dependent insulinotropic polypeptide receptor knockout mice are impaired in learning, synaptic plasticity, and neurogenesis. J Neurophysiol. 2011;105:1574-80.
48. AH S-U, MN G, LS G, CB C, B S, B H*, et al.* GIP(3-30)NH is a potent competitive antagonist of the GIP receptor and effectively inhibits GIP-mediated insulin, glucagon, and somatostatin release. Biochemical pharmacology. 2017;131:78-88.
49. Gasbjerg LS, Hartmann B, Christensen MB, Lanng AR, Vilsboll T, Jorgensen NR*, et al.* GIP's effect on bone metabolism is reduced by the selective GIP receptor antagonist GIP(3-30)NH2. Bone. 2020;130:115079.
50. Sathiya Priya C, Vidhya R, Kalpana K, Anuradha CV. Indirubin-3'-monoxime prevents aberrant activation of GSK-3beta/NF-kappaB and alleviates high fat-high fructose induced Abeta-aggregation, gliosis and apoptosis in mice brain. Int Immunopharmacol. 2019;70:396-407.

Figures

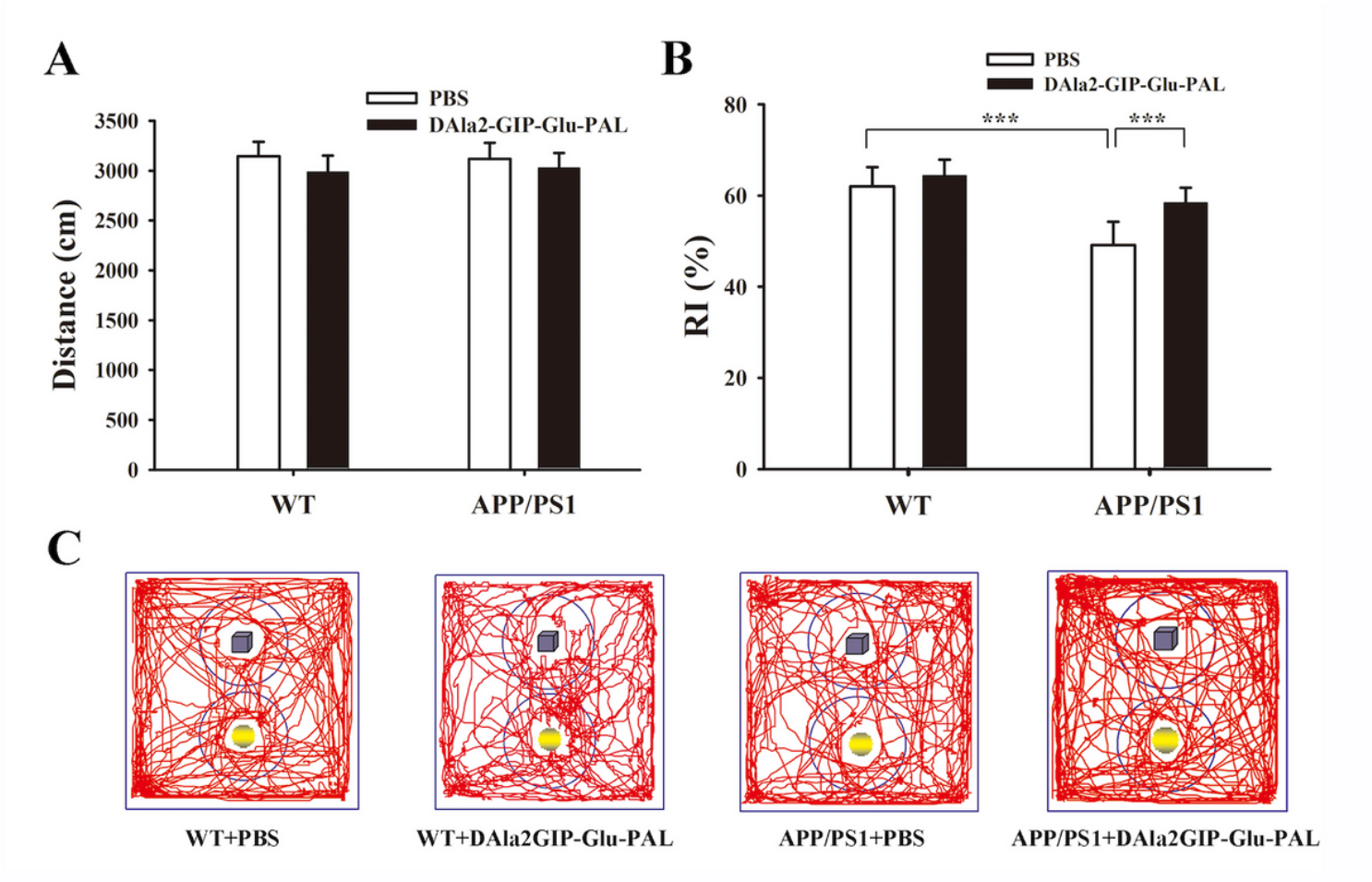

Figure 1

DAla2GIP-Glu-PAL treatment improved new object recognition ability in APP/PS1 mice. A) Histograms showing the total running distance of mice in the open field, no significant difference between groups (n=12 for each group). B) Histograms showing the new object RI of mice. The reduced RI in APP/PS1 mice was significantly reversed by DAla2GIP-Glu-PAL treatment (***P<0.001, n=12 for each group). C) Representative running traces of mice in new object recognition test. The blue cube represents familiar object and the yellow ball represents novel object.

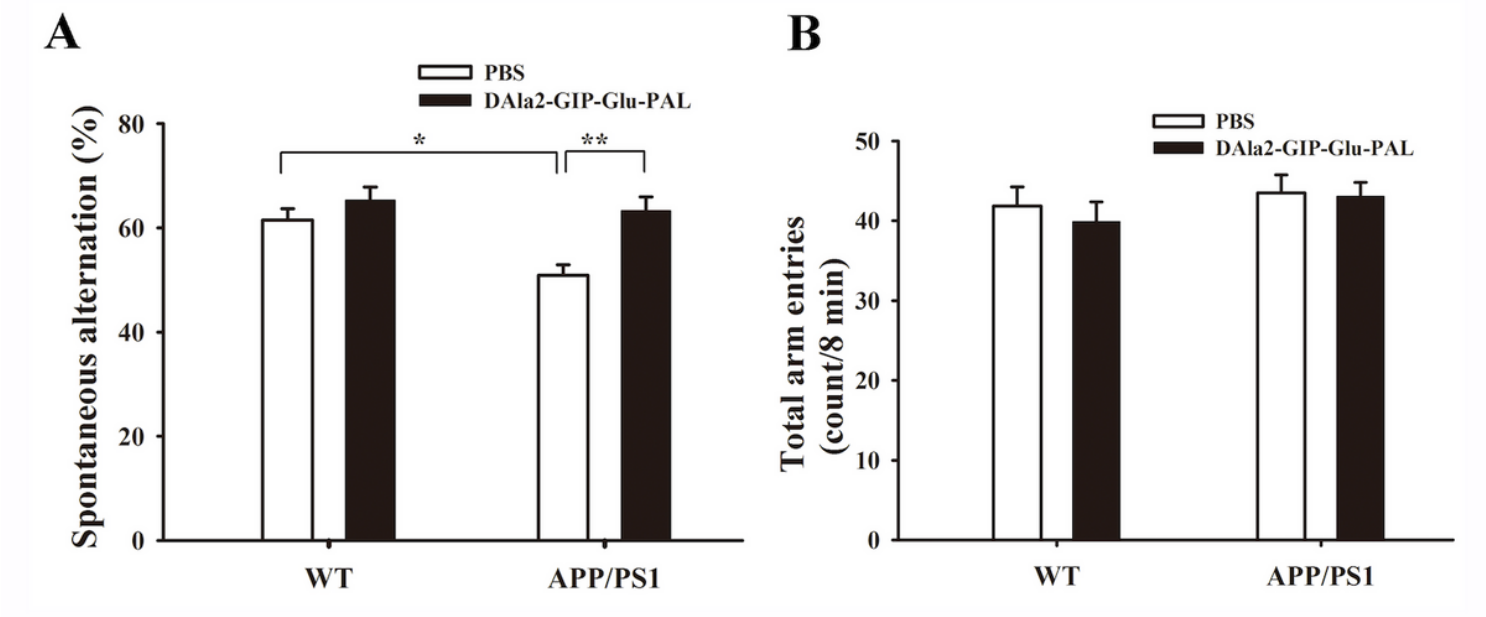

Figure 2

DAla2GIP-Glu-PAL treatment alleviated the working memory deficits of APP/PS1 mice in Y maze test. A) Histograms showing lower spontaneous alternation in the APP/PS1+PBS group and significant recovery after treatment with DAla2GIP-Glu-PAL (*P<0.05, **P<0.01, n=12 for each group). B) Histograms showing no significant difference in total arm entries among the different groups.

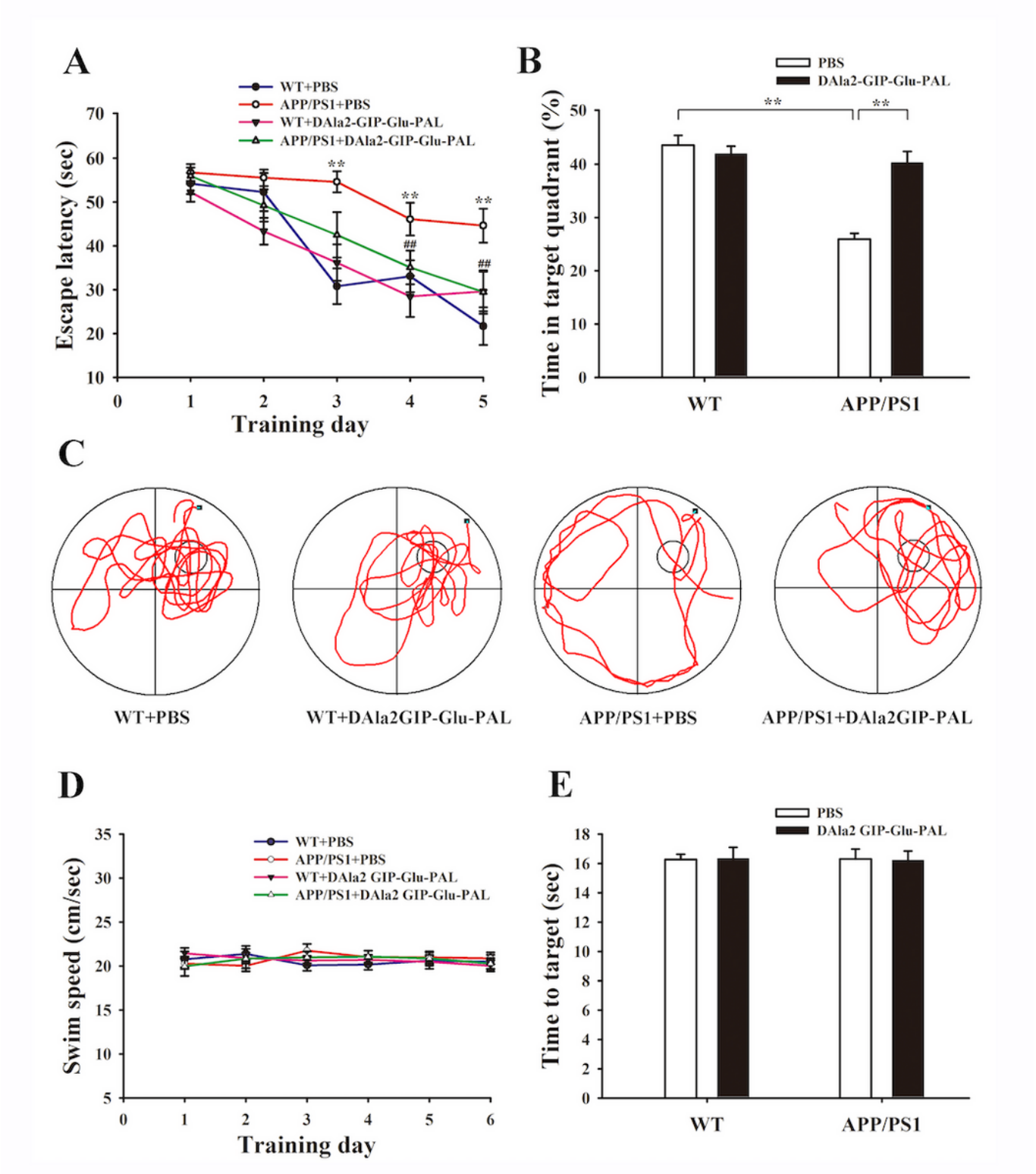

Figure 3

DAla2GIP-Glu-PAL treatment improved spatial learning and memory of APP/PS1 mice. A) Plots showing the changes in average escape latencies of mice in searching for the hidden platform during five consecutive training days (**P<0.01 vs. WT+PBS group; ##P<0.01 vs. APP/PS1+PBS group, n=12 for each group). B) Histograms showing the swimming time percentage of the mice in the target quadrant, with a significant decrease in the APP/PS1-PBS group and a reversal after DAla2GIP-Glu-PAL treatment.

C) Representative swimming traces of mice in the four groups during probe trials. The large circle represents the water maze pool, and the small circle represents the platform. D) Plots showing the changes in the average swim speed of mice during 6 consecutive days, without significant difference between groups (P>0.05). E) Histograms showing the swimming time of mice to visible platform, without significant difference among groups (P>0.05).

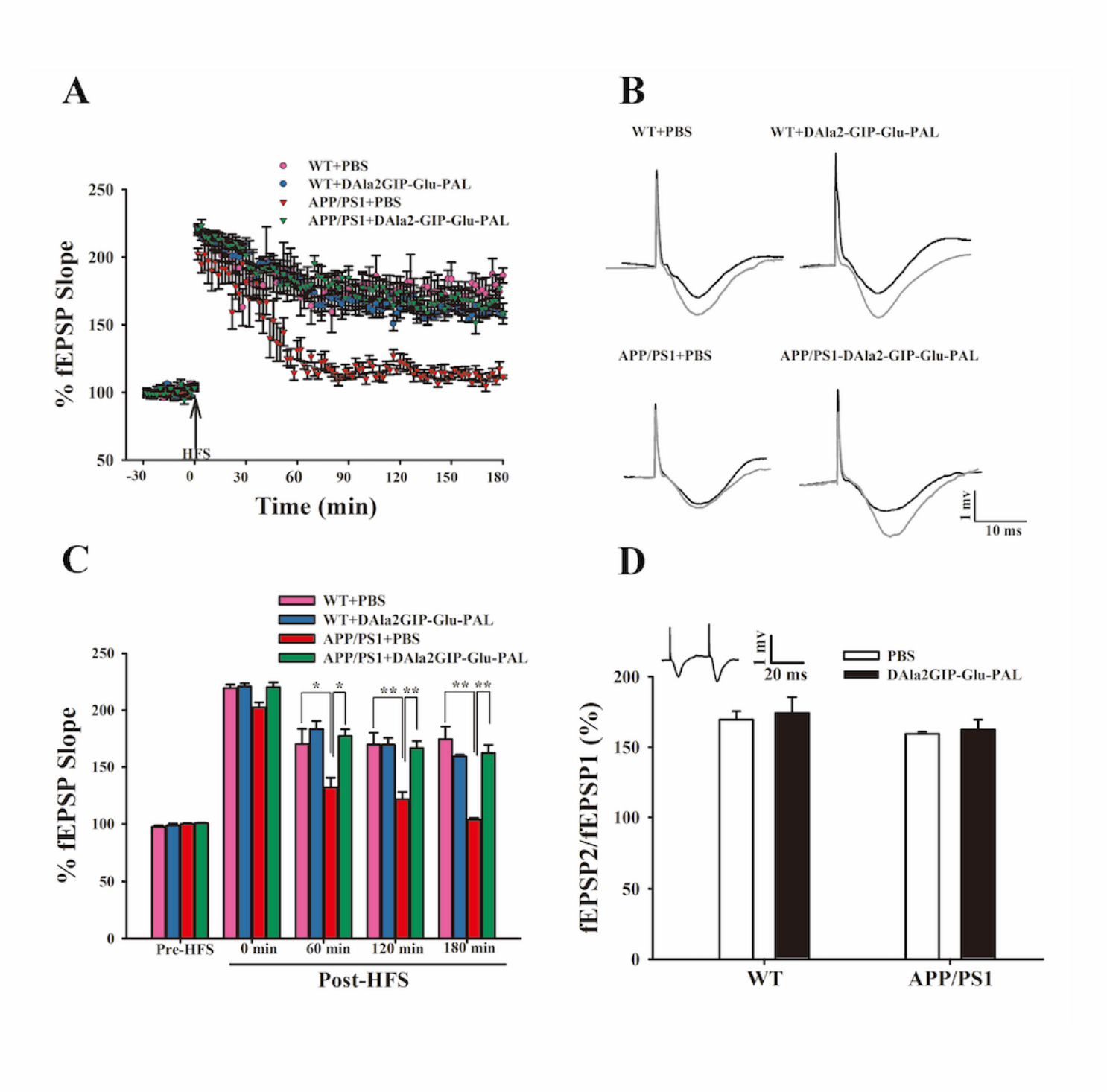

Figure 4

DAla2GIP-Glu-PAL treatment reversed hippocampal L-LTP suppression in APP/PS1 mice. A) Plots showing the test stimuli-induced fEPSPs in the hippocampal CA1 region of APP/PS1 mice before and

after HFS (n = 6-7). B) Typical fEPSP traces recorded before (black line) and 3h after (grey line) HFS in the four groups. Scale bars, 1 mV and 10 ms. C) Histograms showing the normalized fEPSP slope pre-HFS, 0 min, 60 min, 120 min and 180 min post-HFS (*P<0.05 and **P<0.01). D) Histograms showing the ratios of paired pulses in different groups (n = 6–7). Inset: a sample trace of fEPSP induced by paired pulses.

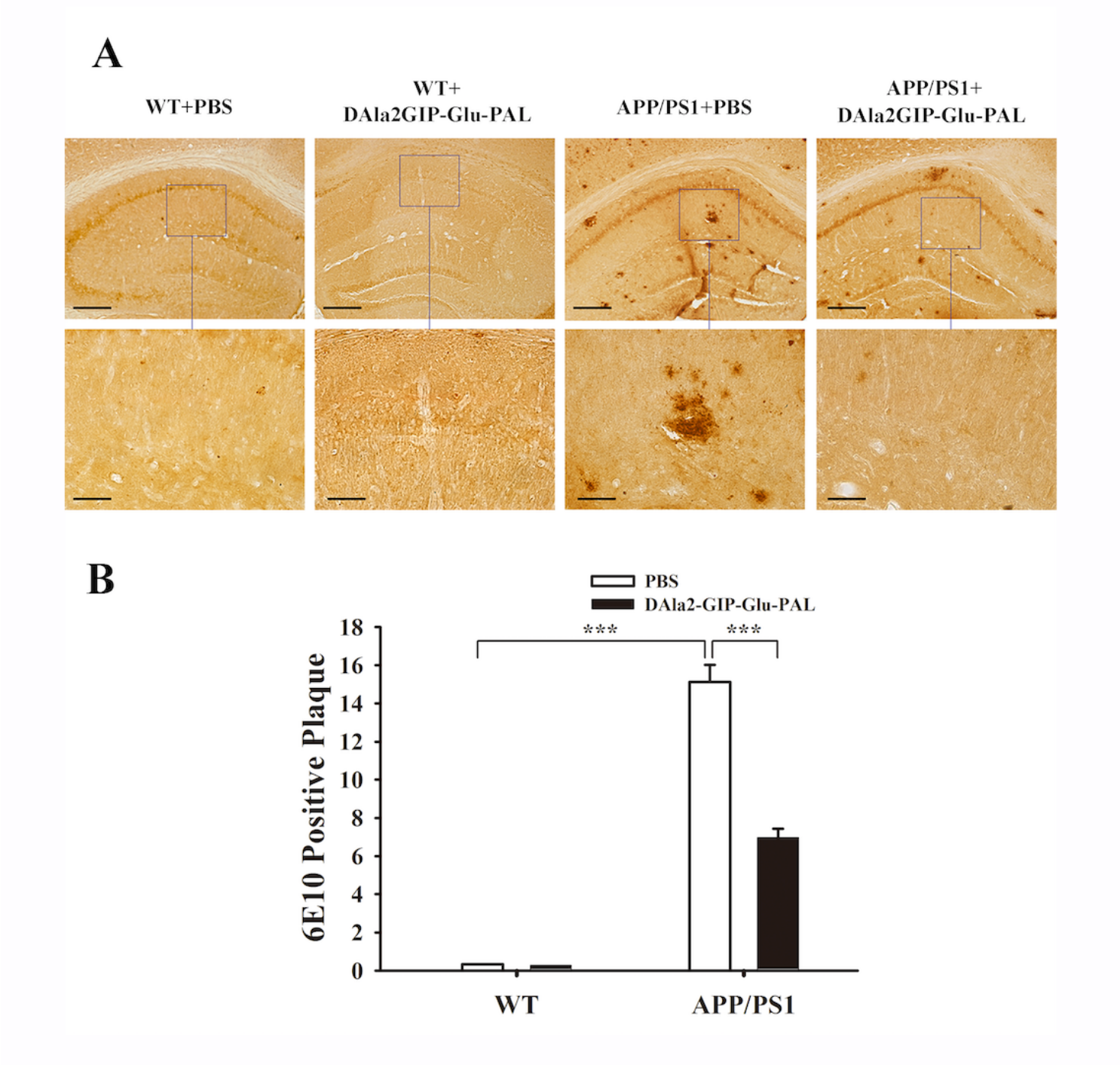

Figure 5

. DAla2GIP-Glu-PAL treatment reduced Aβ plaques in the hippocampus of APP/PS1 mice. A) Photographs showing the distribution of Aβ immunoreactivity-positive plaques in the hippocampus of mice after treatment with DAla2GIP-Glu-PAL or PBS. The bars are 100 μm and 50 μm in the upper and lower rows,

respectively. B) Histograms showing a significant decrease in number of Aβ plaques in the hippocampus of APP/PS1 mice after DAla2GIP-Glu-PAL treatment (***P<0.001).

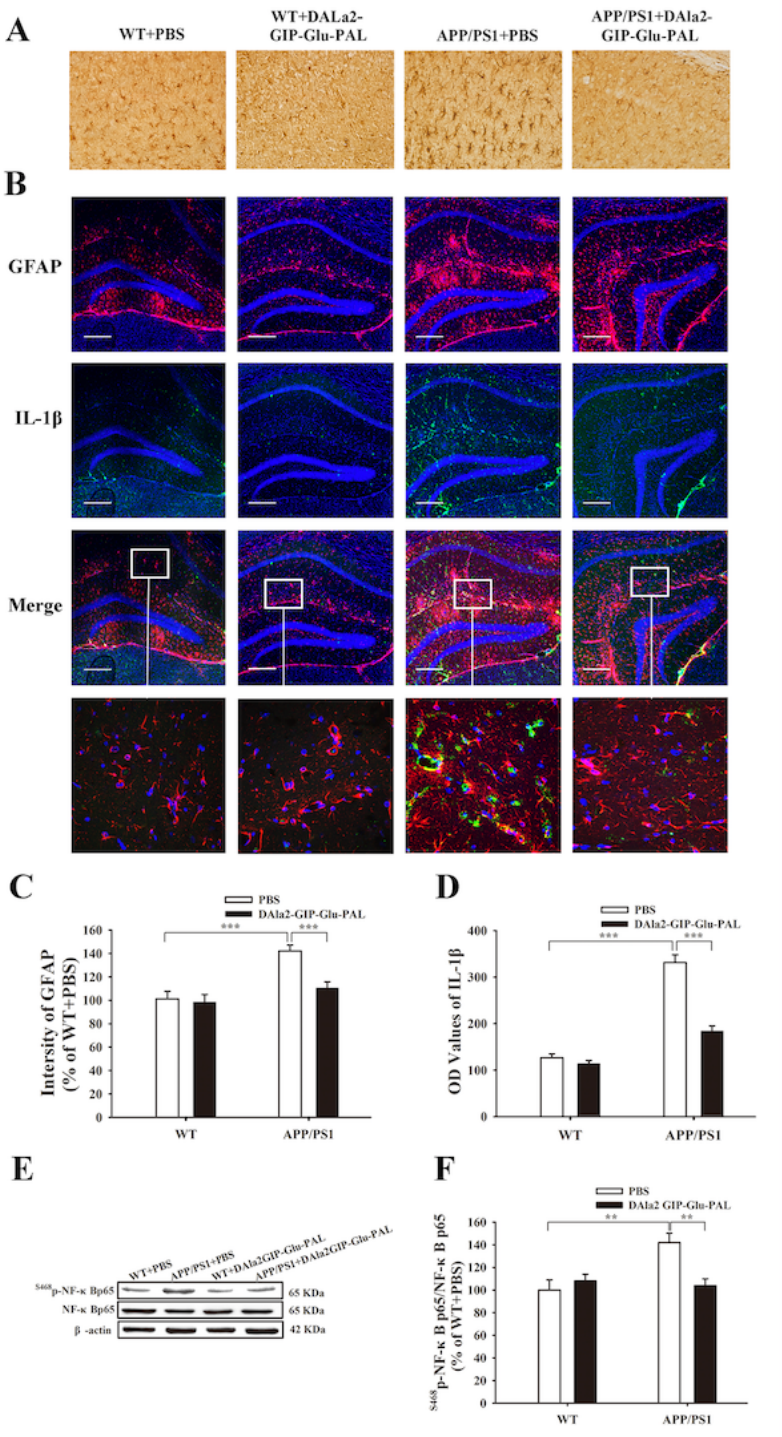

Figure 6

DAla2GIP-Glu-PAL attenuated inflammatory responses in the hippocampus of APP/PS1 mice. A) Photographs showing immunohistochemical staining of GFAP positive cells. Bar=50 μm. B) Photographs showing the immunofluorescence double staining of GFAP (red) and IL-1β (green) positive cells in the

hippocampus. The blue points represent DAPI stained neuronal nuclei. C) Histograms showing that the increased GFAP immunopositive staining in the APP/PS1+PBS mice has a significant decline after DAla2GIP-Glu-PAL treatment (***P<0.001). D) Histograms showing that the increased level of IL-1β measured by ELISA in the APP/PS1+PBS group was significantly decreased by DAla2GIP-Glu-PAL (***P<0.001). E) Representative Western-blotting bands for Ser468p-NF-κBp65. DAla2GIP-Glu-PAL reversed the changes of protein content in the hippocampus of APP/PS1 transgenic mice, and β-actin was an internal reference. F) Histograms showing that the increased level of NF-κBp65 (Ser468) measured by western blot in the APP/PS1+PBS group was significantly decreased by DAla2GIP-Glu-PAL (**P<0.01).

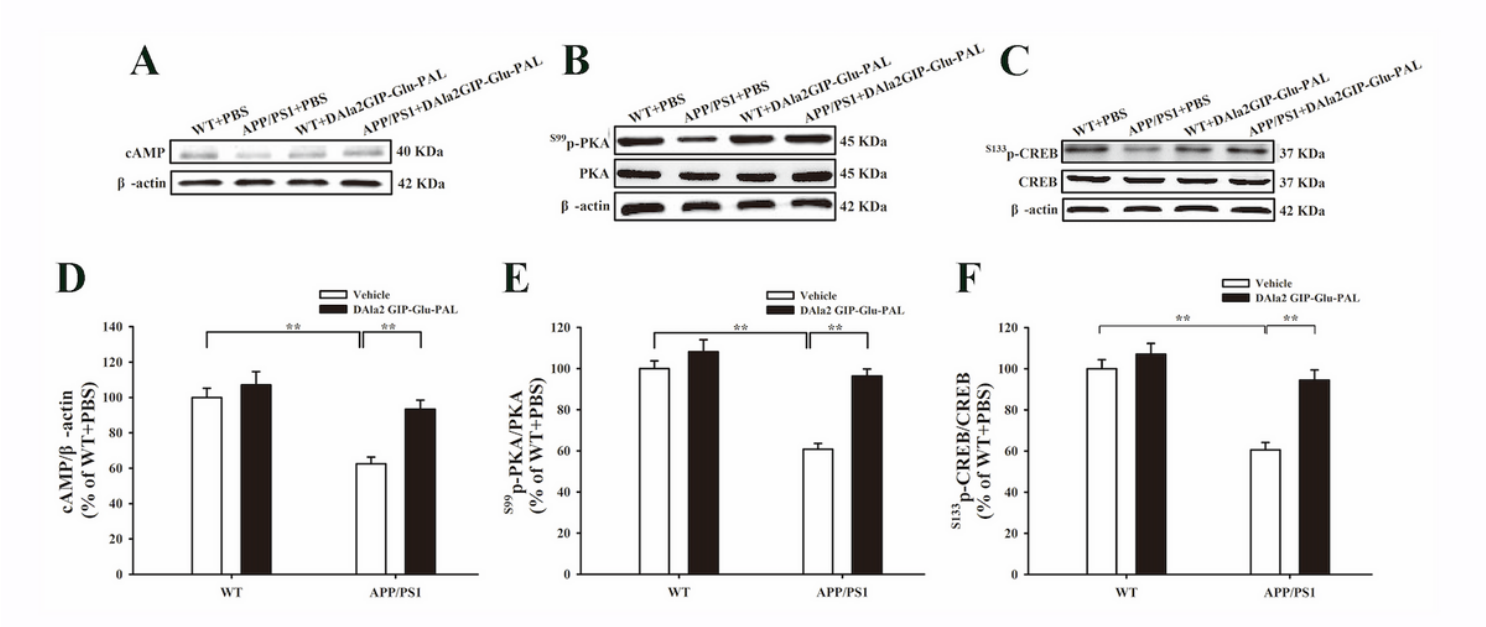

Figure 7

DAla2GIP-Glu-PAL upregulated the levels of cAMP, S99p-PKA and S133p-CREB in hippocampus of mice. A), B) and C) are representative Western-blotting bands for cAMP, S99p-PKA and S133p-CREB in different groups. DAla2GIP-Glu-PAL reversed the changes of protein content in hippocampus of APP/PS1 transgenic mice, and β-actin was an internal reference. D), E) and F) are the statistical histograms of the relative gray values of cAMP, S99p-PKA/PKA and S133p-CREB/CREB protein bands in each group. All values were expressed as percentages of WT+PBS mice. Significance was determined using a two-way ANOVA and post hoc Tukey's multiple comparison tests. **P<0.01.